PROCEEDINGS OF SPIE

SPIEDigitalLibrary.org/conference-proceedings-of-spie

High-performance transparent film heater with an embedded Ni metal-mesh based on selected metal electrodeposition process

Liu, Yanhua, Shen, Su, Chen, LinSen, Zhou, Yun, Ye, Yan, et al.

Yanhua Liu, Su Shen, LinSen Chen, Yun Zhou, Yan Ye, Yanyan Wang, Wen Qiao, Wenbin Huang, "High-performance transparent film heater with an embedded Ni metal-mesh based on selected metal electrodeposition process," Proc. SPIE 10019, Optoelectronic Devices and Integration VI, 100191B (31 October 2016); doi: 10.1117/12.2245975

SPIE.

Event: SPIE/COS Photonics Asia, 2016, Beijing, China

High-performance transparent film heater with an embedded Ni metal-mesh based on selected metal electrodeposition process

Yanhua Liu, Su Shen*, LinSen Chen, Yun Zhou, Yan Ye, Yanyan Wang, Wen Qiao, Wenbin Huang*

College of Physics, Optoelectronics and Energy & Collaborative Innovation Center of Suzhou Nano Science and Technology, Soochow University, Suzhou, 215006, China
Key Lab of Advanced Optical Manufacturing Technologies of Jiangsu Province & Key Lab of Modern Optical Technologies of Education Ministry of China, Soochow University, Suzhou, 215006, China
E-mail: sushen@suda.edu.cn, wbhuang@suda.edu.cn

ABSTRACT

An ultra-flexible and low-sheet resistance transparent conductive film is developed from nickel metal-mesh (Ni metal-mesh) embedded in a polyimide (PI) by exploiting selective deposition technique coupled with photolithography and subsequent inverted film-processing method. The fabricated conductive film achieved sheet resistance values as low as 0.15 Ω sq^{-1}, with corresponding optical transmittance as 80% at 550 nm corresponding the figure of merit up to 1.1×10^4. The film shows excellent adhesion and also preserves its structural integrity and good contact with the substrate for severe bending showing less than 4% decrease of conductivity even after 10^4 cycles. Finally, employing the fabricated Ni metal-mesh/PI conductive film, a hybrid transparent thin-film heater is demonstrated, which exhibited higher heating temperatures (110 ^{o}C) under the lower operating voltage (1 V), lower power consumption (79.1 ^{o}C cm^2 W^{-1}), and shorter response time (T < 2 s) than other heaters, as well as stability after repeated test.

Keywords: Transparent conductive film, flexible electronics, selective electrodeposition, transparent thin-film heater

1. INTRODUCTION

High-quality transparent film heaters (TFHs) are essential component of a broad range of electronics devices including the window defrosters, thermal-based sensors, and outdoor panel displays[1-5]. The most commonly used transparent conductive film indium-thin-oxide (ITO) has been widely used as TFH for its excellent electronic and optic performances [6]. However, film brittleness, high materials cost, low

Optoelectronic Devices and Integration VI, edited by Xuping Zhang, Baojun Li, Changyuan Yu, Proc. of SPIE Vol. 10019, 100191B · © 2016 SPIE
CCC code: 0277-786X/16/$18 · doi: 10.1117/12.2245975

abundance of indium, and optical absorption strongly motivate the alternative materials to substitute ITO [7-10]. Potential alternatives to ITO have been explored including Ag nanowires (AgNWs)[3, 11-13], carbon nanotubes and graphene[2, 14-16], and metal grids[17-19]. The candidate materials used as flexible TFHs should provide uniform current distribution to reach homogeneous temperature field, rapid response and higher temperature at low input power. Among the alternative materials, metal mesh technique has been demonstrated potential in optical transparency, electrical conductivity, and suitable mechanical properties.

TFHs based on AgNWs have been widely reported [11-13]. However, AgNWs deposited on the flexible substrate (e.g., polyethylene terephthalate (PET)) suffer from several problems, such as the delamination of the AgNWs from a flexible substrate, the low thermal-resistance of PET limited the maximum temperature, and non-uniform AgNWs distribution over the substrate. Flexible TFHs comprising AgNWs network embedded in the surfaces of polyimide (PI) have been demonstrated[4]. To reach lower energy consumption, the numbers of AgNWs rod-coating cycles should be increased, which further result in the decrease of transmittance.

Compared with random AgNWs based TFHs, the predesigned metal mesh TFHs with tunable sheet resistance and transmittance become more promising. Here, we introduce an ultra-flexible and low-sheet resistance transparent conductive film, which developed from nickel metal mesh (Ni metal mesh) embedded in a polyimide (PI) by exploiting selective deposition technique coupled with photolithography and subsequent inverted film-processing method. The novel fabrication process exploits a metal selective electrodeposition technique to substitute vacuum-based metal deposition, which is crucial for low-cost, large-area devices fabrication. The Ni metal mesh based TFHs exhibited higher heating temperatures (110 ^{o}C) under the lower operating voltage (1 V), lower power consumption (79.1 ^{o}C cm^{2} W^{-1}), and shorter response time (T < 2 s) than other TFHs.

2. EXPERIMENTAL PROCEDURES

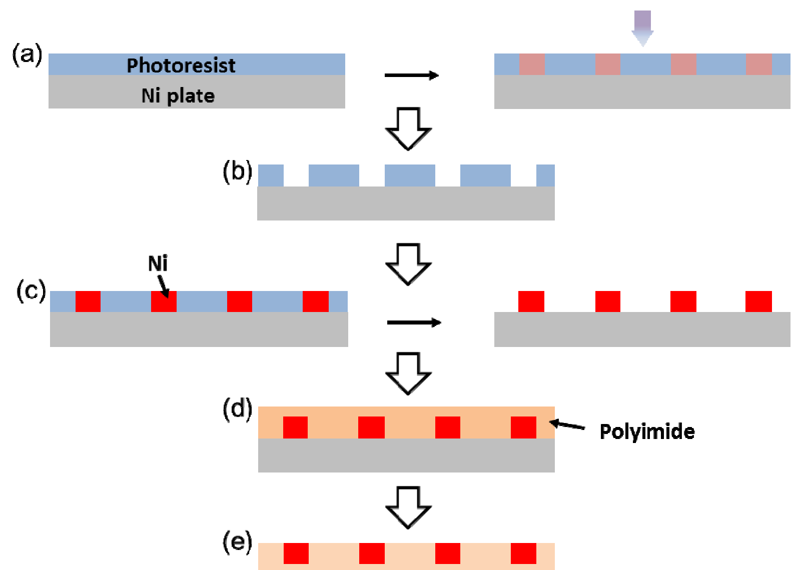

Figure1. Schematic illustration of the fabrication of TFHs based on the embedded Ni mesh on PI substrate. Fabrication of patterned microgrooves on the photoresist by photolithography. (a) Spin-coating the photoresist layer on Ni plate and generated pattern by photolithography. (b) Microgrooves pattern on Ni plate. (c) Deposed Ni into micro-trenches and then remove the photoresist. (d) Spin-coating the PI solution on Ni substrate and bake for evaporating solvent. (e) Peel off the substrate and obtain Ni mesh/PI TFHs.

The embedded Ni mesh/PI composited conductors are introduced as a high performance TFH and the fabricated process is depicted in Figure. 1 (a) – (f). Firstly, a layer of photoresist (RAJ-3090PG, Ruihong Electronic Chemical Co., LTD) is spin coated on the Ni plate substrate, then the arbitrary microgrooves are directly written on photoresist with a digital micro-mirror devices (DMD) based maskless photolithography (iGrapher200, SVG DigitOPtics, Co., LTD). Upon development in NaOH (0.6%) solution for 10 s and subsequent drying in the air, the microgrooves generate on the Ni plate substrate. Secondly, Ni deposited and filled inside the microgrooves defined by photoresist, though the selective deposition process. After removal of the photoresist, the bare Ni metal mesh stands on the surface of the Ni plate. The confocal microscopy images of the Ni mesh measured by 3D laser con-focal microscopy (Keyence, VK 9700) are illustrated in Figure. 2. The diagonal length of hexagonal Ni mesh is 50 μm, and its thickness and width is 1.5 μm and 3.5 μm, respectively.

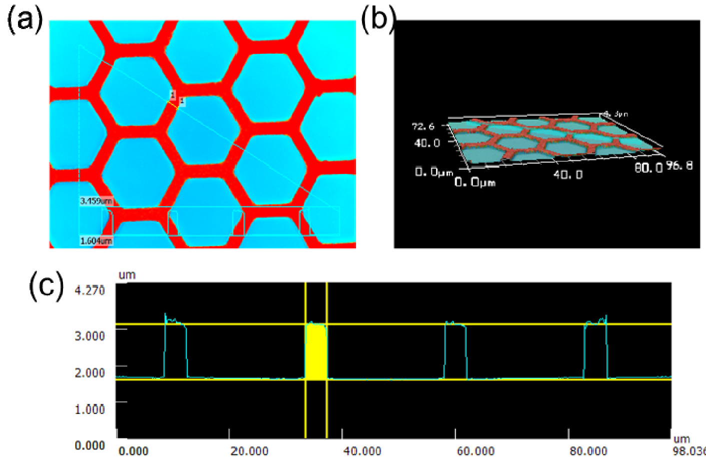

Figure 2. Experiment realization of the bare Ni mesh structure on the Ni plate. The three-dimensional confocal microscopy images of top-view (a) and bird-view (b) and thickness profile (c) of the hexagonal Ni mesh (period of 50 μm, thickness of 1.5 μm, and width of 3.5 μm).

Subsequently, transparent PI solution (POMESci-tech Co., LTD) was cast on the Ni mesh, and then placed on the oven to evaporate the solvent. After drying 1 h at 50 ^{o}C, subject to the procedure heating at 80 ^{o}C for 2 h, 150 ^{o}C for 1 h, and 200 ^{o}C for 2 h. Following the annealing, the fabricated PI film with thickness about 20 μm. Finally, the PI film embedded Ni mesh was peeled off from the Ni plate substrate. Figure 3 shows a three-dimensional confocal microscopy and scanning electronic microscope (SEM) images for the Ni mesh/PI composite TFH, observed by field emission scanning electron microscopy (FESEM: JEOL, JSM-5400, USA). The surfaces morphology indicated that the PI solution permeated the Ni network well.

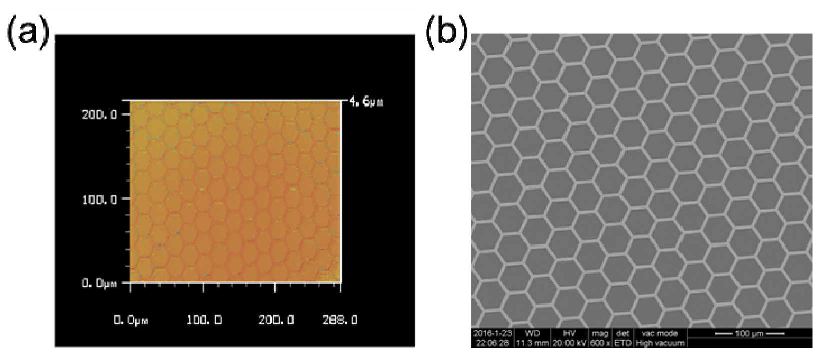

Figure 3. Photo of the Ni mesh/PI TFHs. (a) The three-dimensional confocal microscopy image of the Ni mesh/PI TFHs. (b) SEM picture of the Ni mesh/PI TFHs (scale bar, 100 μm).

3. RESULTS AND DISCUSSION

To evaluate the performance as a transparent conductor, different periodically hexagonal Ni mesh arrays are exploited. In which the Ni mesh embedded in the PI, with period range from 50 to 200 μm, width of 3 μm and height of 3 μm, respectively. The transmittance measured using a UV–vis spectrophotometer (UV-2550, SHIMADZU) are illustrated in the Figure. 4 (a), whose values range from 68% to 88% in the whole visible region. The thickness of the metal affects the sheet resistance even under given period. The sheet resistance values measured 0.15 Ω sq^{-1} (4-point probe, CMT SR2000, A.I.T.) when the metal thickness increased to 3μm with 150 μm period of hexagonal Ni mesh. Correspondingly, the figure of merit of the Ni mesh/PI conductor reach 1.1×10^4 at transmittance of 80%. To further evaluate the mechanical stability of the Ni mesh TFH, a cyclic bending test is performed, as shown in Figure 4(b). The results clearly indicate that no noticeable change in sheet resistance ($(R - R_{initial})/R_{initial} \approx 4\%$), in which the symbols R and $R_{initial}$ are the actual resistance and initial sheet resistance, respectively. It demonstrates the high tolerances of the Ni mesh/PI TFH to the bending stress. The Ni mesh/PI TFH can maintain its electrical performance under bending for up to 10000 cycles. However, the ITO transparent conductor's resistance increases significantly after 500 bending cycles due to the material brittleness.

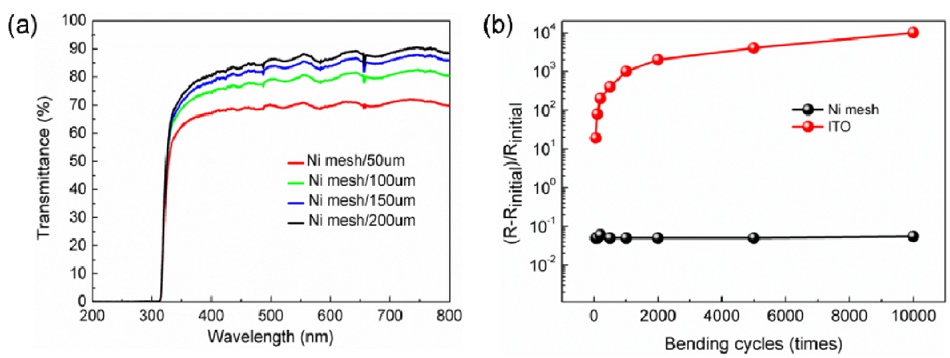

Figure 4. (a) Transmittance spectra of the Ni mesh/PI TFHs with 50, 100, 150, 200μm diagonal length as the function of wavelength, respectively. (b) Change of sheet resistance versus bending cycles for bendable TFH consisting of Ni mesh and ITO films on 200-μm-thick PET substrates.

To investigate the performance of the composited Ni mesh/PI TFH, the temperature properties of the TFH were analyzed. The $1cm\times1cm$ Ni mesh/PI TFH with sheet resistance of 0.15Ω sq^{-1} employed in the experiment. The temperature properties of the TFH are depicted in Figure. 5(a), which are measured under various applied voltages (range from 0.2V to 1V). The maximum temperature of the TFH can reach above 110°C when the applied voltage increased to 1V, demonstrating its well performance at a low input voltage. The steady-state temperature of the TFH can be reached within 2 s, and then cool to ambient temperature when no voltage signal applied within the same time. The steady-state temperature of the TFH as a function of the input power is shown in Figure. 5(b). Considering the size of the TFH, the electrical power consumption of the device can be calculated to be 79.1 ^{o}C cm^{2} W^{-1}. The results demonstrated the TFH based on Ni mesh/PI can operate at low input voltages and require low power consumption, which is attributing to the low sheet resistance of the Ni mesh/PI conductor. Meanwhile the stability tests under 1 V showed no significant degradation of maximum temperature as depicted in Figure. 5(c), which is essential for the repeated use.

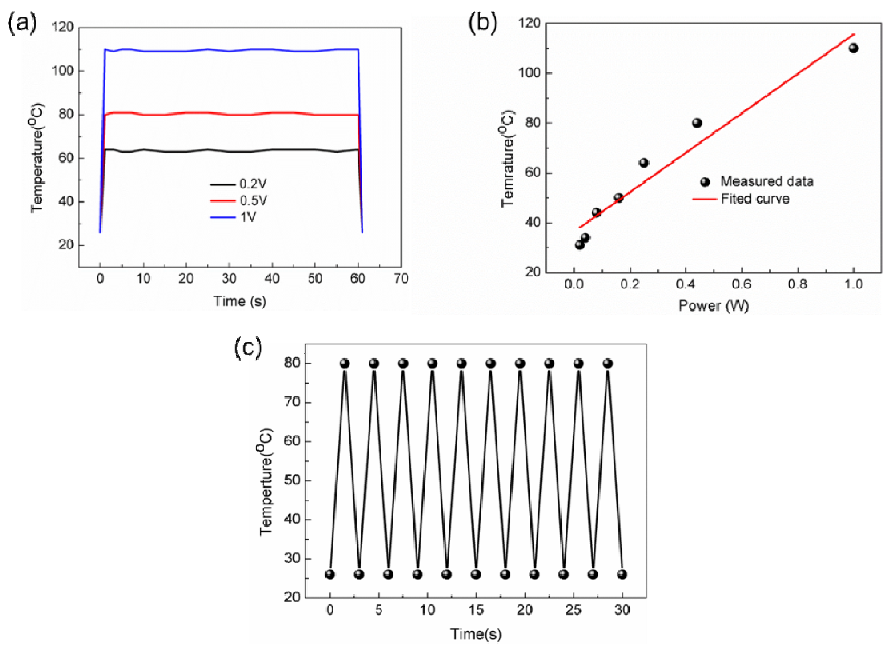

Figure 5. Characterization of the fabricated Ni mesh/PI TFHs. (a) Temperature profiles of the Ni mesh/PI TFH with sheet resistance 0.15Ω sq^{-1} versus time under different applied voltages. (b) The steady state temperature of the Ni mesh/PI TFH as the function of the input power. (c) Cycling performance of Ni mesh/PI TFH with sheet resistance of 0.15Ω sq^{-1}.

4. CONCLUSION

In conclusion, we have demonstrated an innovative flexible TFH based on Ni mesh/PI with good bending capability, low operating voltage, fast response time, and low power consumption. The Ni mesh/PI conductors, fabricated by selective deposition technique coupled with photolithography and subsequent inverted film-processing method, have lower sheet resistance in comparison with other existing flexible electrodes at a given transparency, which is beneficial to realization well performance TFHs. By combining superior performance and the low-cost, large-area fabrication process, our results demonstrated the TFH based on metal mesh/PI hybrid conductive film has broad applications in flexible and stretchable optoelectronic devices.

ACKNOWLEDGMENT

This work is supported by the National Natural Science Foundation of China (NSFC) (61405133, 61575133, 51302179, 91323303), and by the Specialized Research Fund for the Doctoral Program of Higher Education (No. 20133201120027), and by the Natural Science Foundation of Jiangsu Province (No. BK20140348), and by a project funded by the Priority Academic Program Development (PAPD) of Jiangsu Higher Education Institutions.

REFERENCES

[1]Y. H. Yoon, J. W. Song, D. Kim, J. Kim, J. K. Park, S. K. Oh, and C. S. Han, "Transparent Film Heater Using Single-Walled Carbon Nanotubes," Adv. Mater. 19(23), 4284-4287 (2007).

[2]J. Kang, H. Kim, K. S. Kim, S.-K. Lee, S. Bae, J.-H. Ahn, Y.-J. Kim, J.-B. Choi, and B. H. Hong, "High-performance graphene-based transparent flexible heaters," Nano Lett. 11(12), 5154-5158 (2011).

[3]T. Kim, Y. W. Kim, H. S. Lee, H. Kim, W. S. Yang, and K. S. Suh, "Uniformly interconnected silver-nanowire networks for transparent film heaters," Adv. Funct. Mater. 23(10), 1250-1255 (2013).

[4]Q. Huang, W. Shen, X. Fang, G. Chen, J. Guo, W. Xu, R. Tan, and W. Song, "Highly flexible and transparent film heaters based on polyimide films embedded with silver nanowires," RSC Adv. 5(57), 45836-45842 (2015).

[5]B. Han, Y. Huang, R. Li, Q. Peng, J. Luo, K. Pei, A. Herczynski, K. Kempa, Z. Ren, and J. Gao, "Bio-inspired networks for optoelectronic applications," Nature Comm. 5, 5674 (2014).

[6]K. Im, K. Cho, J. Kim, and S. Kim, "Transparent heaters based on solution-processed indium tin oxide nanoparticles," Thin Solid Films 518(14), 3960-3963 (2010).

[7]P.-C. Hsu, S. Wang, H. Wu, V. K. Narasimhan, D. Kong, H. R. Lee, and Y. Cui, "Performance enhancement of metal nanowire transparent conducting electrodes by mesoscale metal wires," Nature Comm. 4, 2522 (2013).

[8]B. Han, K. Pei, Y. Huang, X. Zhang, Q. Rong, Q. Lin, Y. Guo, T. Sun, C. Guo, and D. Carnahan, "Uniform self-forming metallic network as a high-performance transparent conductive electrode," Adv. Mater. 26(6), 873-877 (2014).

[9]Q. Xu, W. Shen, Q. Huang, Y. Yang, R. Tan, K. Zhu, N. Dai, and W. Song,

"Flexible transparent conductive films on PET substrates with an AZO/AgNW/AZO sandwich structure," J. Mater. Chem. C 2(19), 3750-3755 (2014).

[10]J. Song, S. A. Kulinich, J. Li, Y. Liu, and H. Zeng, "A General One-Pot Strategy for the Synthesis of High-Performance Transparent-Conducting-Oxide Nanocrystal Inks for All-Solution-Processed Devices," Angew. Chem. 127(2), 472-476 (2015).

[11]L. Hu, H. S. Kim, J.-Y. Lee, P. Peumans, and Y. Cui, "Scalable coating and properties of transparent, flexible, silver nanowire electrodes," ACS nano 4(5), 2955-2963 (2010).

[12]I. K. Moon, J. I. Kim, H. Lee, K. Hur, W. C. Kim, and H. Lee, "2D graphene oxide nanosheets as an adhesive over-coating layer for flexible transparent conductive electrodes," Sci. Rep. 3, (2013).

[13]P.-C. Hsu, X. Liu, C. Liu, X. Xie, H. R. Lee, A. J. Welch, T. Zhao, and Y. Cui, "Personal thermal management by metallic nanowire-coated textile," Nano Lett. 15(1), 365-371 (2014).

[14]J. S. Woo, J. T. Han, S. Jung, J. I. Jang, H. Y. Kim, H. J. Jeong, S. Y. Jeong, K.-J. Baeg, and G.-W. Lee, "Electrically robust metal nanowire network formation by in-situ interconnection with single-walled carbon nanotubes," Sci. Rep. 4, (2014).

[15]Z. P. Wu, and J. N. Wang, "Preparation of large-area double-walled carbon nanotube films and application as film heater," Physica E 42(1), 77-81 (2009).

[16]D. Sui, Y. Huang, L. Huang, J. Liang, Y. Ma, and Y. Chen, "Flexible and transparent electrothermal film heaters based on graphene materials," Small 7(22), 3186-3192 (2011).

[17]Y. Jang, J. Kim, and D. Byun, "Invisible metal-grid transparent electrode prepared by electrohydrodynamic (EHD) jet printing," J. Phy. D: Appl. Phy. 46(15), 155103 (2013).

[18]N. Kwon, K. Kim, J. Heo, I. Yi, and I. Chung, "Study on Ag mesh/conductive oxide hybrid transparent electrode for film heaters," Nanotechnology 25(26), 265702 (2014).

[19]A. Khan, S. Lee, T. Jang, Z. Xiong, C. Zhang, J. Tang, L. J. Guo, and W. D. Li, "High-Performance Flexible Transparent Electrode with an Embedded Metal Mesh Fabricated by Cost-Effective Solution Process," Small 12(22), 3021-3030 (2016).